

# The environment of active objects in the nearby universe

Georgina V. Coldwell<sup>\*</sup>, Héctor J. Martínez<sup>†</sup> and Diego G. Lambas<sup>‡</sup>

*Grupo de Investigaciones en Astronomía Teórica y Experimental (IATE), Observatorio Astronómico, Universidad Nacional de Córdoba, Laprida 854, 5000, Córdoba, Argentina.*  
*e-mail: georgina@oac.uncor.edu, julian@oac.uncor.edu, dgl@oac.uncor.edu*

29 October 2018

## ABSTRACT

We study the galaxy environment of active galaxies, radio-loud and radio-quiet quasars in the redshift range  $0.1 \leq z \leq 0.25$ . We use APM galaxies in order to explore the local galaxy overdensity and the  $b_J - R$  colour distribution of neighbouring galaxies of these target samples. For comparison, we perform similar analysis on samples of Abell clusters with X-ray emission, and samples of Abell clusters with richness  $R = 1$  and  $R = 0$ . The projected cross-correlations show that the samples of quasars and active galaxies reside in regions of galaxy density enhancements lower than those typical of  $R = 0$  clusters. We also find that in the nearby universe the local galaxy overdensity of radio-loud and radio-quiet quasars are comparable. The analysis of the distribution of  $b_J - R$  galaxy colour indexes suggests that the environment of quasars is not strongly dominated by a population of red galaxies, characteristic of rich Abell cluster, an effect that is more clearly appreciated for our sample of radio-loud quasars.

**Key words:** quasars: clustering— quasars: statistics— quasars: distribution – galaxies: clusters: general – galaxies: distribution

## 1 INTRODUCTION

Studies of the environment of quasars have been the subject of several works in recent years. Some of the analysis in the local universe,  $z < 0.6$ , suggest that quasars reside in groups (Fisher et al 1996), or in clusters (Smith et al 1999, Mc. Lure & Dunlop 2000). However, Martínez et al. (1999) using a quasar-galaxy cross-correlation analysis suggest that high density environments may not be representative of the typical quasar neighbourhood at low redshifts.

At higher redshifts,  $z > 0.6$ , some authors have found evidence of a different environment for radio-loud and radio-quiet quasars (Yee & Green 1987, Yee 1990). Radio-loud quasars being associated mainly with rich Abell clusters while radio-quiet quasars residing either in groups or in the outskirts of clusters. However, more recent studies by Wold et al. (2000, 2001) and Best (2000) cast considerable doubts on previous results since these new analysis do not show any appreciable difference between the typical galaxy overdensity around radio-loud and radio-quiet quasars.

The discussion about the influence of quasar activity on the formation and evolution of galaxies has continued during

the last decades. The possibility that the surrounding galaxies could be responsible for triggering and fueling the quasars was first suggested by Toomre & Toomre (1972). Interacting galaxies and mergers are efficient means of transporting gas into the inner regions of the host galaxy. On the other hand, the large range of influence of a quasar may have implications for structure formation. According to Rees (1988) and Babul & White (1991) quasars may ionize the surrounding medium up to several megaparsecs away. A different approach is adopted by other authors (see for instance Voit 1996 and Silk & Rees 1998), where a fraction of the energy released by quasars is transferred via energetic outflows to the gaseous medium.

In this paper we attempt a characterization of the environment of quasars and active galaxies in the nearby universe by considering the galaxy density enhancement using cross-correlation analysis with APM galaxies. We also use the distribution of  $b_J - R$  colours of neighbouring galaxies to explore their stellar population properties and deepen our understanding of nuclear activity and galaxy formation and evolution. In section 2 we describe the data, section 3.1 deals with the cross-correlation analysis, section 3.2 with the relative distribution of  $b_J - R$  colour indexes of APM galaxies around the different target samples. Finally, section 4 provides a brief discussion of the main results.

<sup>\*</sup> On a fellowship from Agencia Córdoba Ciencia, Córdoba, Argentina

<sup>†</sup> CONICET fellow, Argentina

<sup>‡</sup> CONICET, Argentina

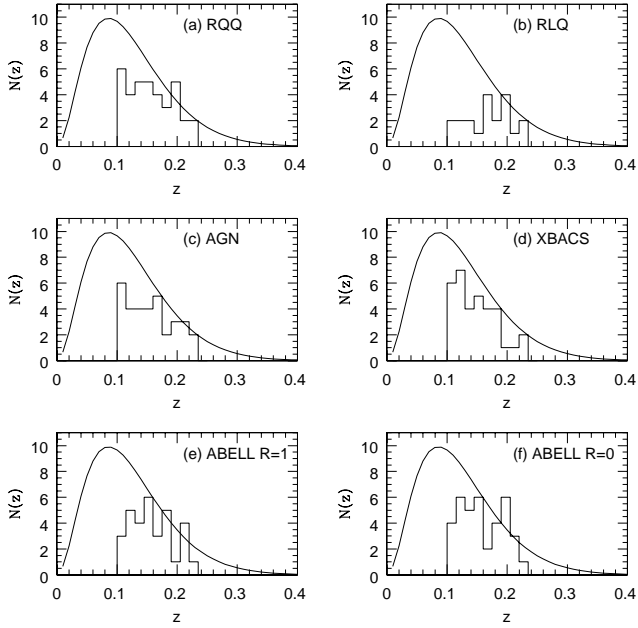


**Figure 1.** Redshift distributions of the different samples. The smooth curve represents the expected redshift distribution for APM galaxies with limiting apparent magnitude  $b_J^{\text{lim}} = 20.5$  as derived by Baugh & Efstathiou (1993).

## 2 DATA

The active object target samples used in this work consist in radio-loud quasars, hereafter RLQs, radio-quiet quasars, hereafter RQQs, and active galaxies, hereafter AGNs, from the Quasars and Active Galactic Nuclei 9th Ed. Catalog (Véron-Cetty & Véron 2000). The cluster targets consist in clusters of galaxies taken from the X-ray Bright Abell Cluster Sample (XBACS) (Ebeling et al. 1996) and Abell clusters with richness  $R = 1$  and  $R = 0$  selected from Abell et al. (1989).

All target samples have been restricted to the redshift range  $0.1 \leq z \leq 0.25$  taking into account the similarity of the target redshift distributions within this range, and the large amplitude of correlation of the targets with APM galaxies. Tracer galaxies within  $0.5^\circ$  of the targets were taken from the APM Southern Sky Catalogues (<http://www.ast.cam.ac.uk/~apmcat/>) and restricted to those targets for which data in the two bands  $b_J$  and  $R$  are available. The final number of targets in each sample are listed in Table 1. The samples of Abell clusters were restricted to richness  $R \leq 1$  to avoid the inclusion of clusters already considered in the XBACS sample since XBACS include mostly  $R \geq 2$  clusters.

We have also considered 30 randomly selected fields to make an appropriate comparison with the mean background properties. Main characteristics of the target samples analysed are also listed in Table 1.

The different target samples have similar redshift distributions as it can be seen in Figure 1, so that the results of our analysis are not subject to different  $K$ -correction effects as well as other possible systematic that depend on sample depth. For comparison, in each panel of Figure 1 is shown

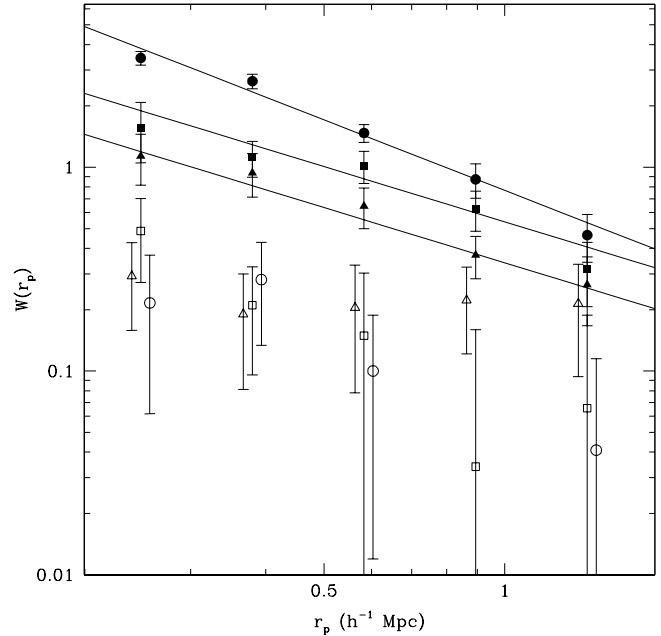


**Figure 2.** Projected Cross-Correlation Functions. Filled circles correspond to XBACS cluster sample, filled squares correspond to Abell  $R = 1$  and filled triangles to Abell  $R = 0$ . The best fit power-law to the projected cross-correlation function for the cluster samples are shown (see parameters in text). Empty squares correspond to RLQs, empty triangles to RQQs and empty circles to AGNs.

the expected redshift distribution of APM tracer galaxies for a limiting apparent magnitude  $b_J^{\text{lim}} = 20.5$  (see Baugh & Efstathiou 1993) in arbitrary units.

## 3 ANALYSIS

### 3.1 Galaxy overdensities around the targets

In order to make a suitable characterisation of the typical galaxy density enhancement around the objects in the selected samples, we computed the cross-correlation functions for centers of the different target samples and APM tracers with a limiting magnitude  $b_J^{\text{lim}} = 20.5$ . Since all center targets in our samples have measured redshifts, we are able to compute cross-correlations as a function of projected distance which improves the information obtained from angular correlations.

We have used the following estimator of the two-point correlation function:

$$W(r_p) = \frac{DD(r_p)N_R}{DR(r_p)N_D} - 1, \quad (1)$$

where  $DD(r_p)$  and  $DR(r_p)$  are the number of target-galaxy and target-random point pairs respectively, separated in each case by a projected distance  $r_p$  in the interval  $[r_p - \Delta r_p, r_p + \Delta r_p]$ ,  $N_D$  and  $N_R$  are the number of objects in the data and random catalogs respectively. When computing projected distances we have assumed a flat cosmology ( $q_0 = 0.5$ ) and a Hubble constant  $H_0 = 100 \text{ h km s}^{-1} \text{ Mpc}^{-1}$ .

**Table 1.** Target sample characteristics.

Sample	Number of objects	Source	Main characteristics
RQQs	41	Véron-Cetty & Véron (2000)	$M_B \leq -23$ , radio-quiet
RLQs	19	Véron-Cetty & Véron (2000)	$M_B \leq -23$ , radio-loud
AGNs	35	Véron-Cetty & Véron (2000)	$M_B > -23$
XBACS	34	Ebeling et al. (1996)	$F_{lim} = 5.0 \times 10^{-12} \text{ erg cm}^{-2} \text{ s}^{-1}$
Abell $R = 1$	35	Abell et al. (1989)	$R = 1$
Abell $R = 0$	45	Abell et al. (1989)	$R = 0$

The resulting cross-correlation functions are shown in Figure 2. Error bars in these figures were estimated with the bootstrap resampling technique (Barrow et al. 1984) with 30 bootstrap samples.

In Figure 2 we show the projected cross-correlation functions corresponding to the three cluster samples and the samples of active objects, where it can be seen the decrease of the cross-correlation amplitude moving from richer to poorer clusters as well as the lack of strong correlation for the samples of active objects. It is clear that the projected cross-correlation functions of the samples of active objects have systematically lower amplitude than those of cluster samples (even  $R = 0$ ) and they are indistinguishable taking into account uncertainties.

Assuming a power-law model for the spatial correlation function,  $\xi(r) = (r/r_0)^{-\gamma}$ , the projected correlation function is

$$W(r_p) = C\pi^{1/2} \frac{\Gamma((\gamma-1)/2)}{\Gamma(\gamma/2)} \frac{r_0^\gamma}{r_p^{(\gamma-1)}}. \quad (2)$$

where the constant  $C$ ,

$$C = \frac{\sum_i p(y_i)}{\sum_i \left(\frac{1}{y_i^2}\right) \int_0^\infty p(x)x^2 dx}, \quad (3)$$

takes into account the probability  $p(x)$  for a tracer galaxy to be found at a distance  $x$  from the observer and is derivable from the galaxy luminosity function  $\phi(L)$ :

$$p(x) \propto \int_{L_{\min}(x)}^\infty \phi(L) dL, \quad (4)$$

where a galaxy at a distance  $x$  must have a luminosity greater than  $L_{\min}(x)$  to be included in the tracer sample (see Lilje & Efstathiou 1988). In equation (3)  $y_i$  is the radial distance to the  $i$ -th center target. We have used a Schechter fit to the luminosity function (Schechter 1976) for the tracer galaxies with parameters  $M_{b_J}^* = -19.7 + 5 \log h$ ,  $\alpha = -1.0$  and we have included a linear  $K$ -correction,  $K = 3z$ , in computing  $L_{\min}(x)$ . By fitting power-laws to the cross-correlation functions we have inferred slopes and correlation lengths for the cluster samples. We obtain  $\gamma = 2.09 \pm 0.09$ ,  $r_0 = (11 \pm 2)h^{-1}\text{Mpc}$  for XBACS;  $\gamma = 1.9 \pm 0.2$ ,  $r_0 = (11 \pm 3)h^{-1}\text{Mpc}$  for Abell  $R = 1$ ;  $\gamma = 1.9 \pm 0.2$ ,  $r_0 = (9 \pm 2)h^{-1}\text{Mpc}$  for Abell  $R = 0$ .

The low amplitude and the large error bars of the cross-correlations of active objects do not allow adequate power-law fits. A useful quantity to characterise the typical galaxy overdensity around the center targets considers the number of tracer galaxies at projected distances  $r_p \leq 1h^{-1}\text{Mpc}$  with respect to the random fields,

$$N_{TARGET}^{\text{excess}} = \langle N \rangle - N_{RAN} \quad (5)$$

Our sample of tracer galaxies are limited to  $b_J \leq 20.5$  and corresponds to objects brighter than  $M_{b_J} = -17.7 + 5 \log h$  at  $z \sim 0.15$ . We find for active objects  $N_{AGNs}^{\text{excess}} \sim 15$ ;  $N_{RQQs}^{\text{excess}} \sim 13$ ;  $N_{RLQs}^{\text{excess}} \sim 10$ . For clusters we find  $N_{XBACS}^{\text{excess}} \sim 100$ ;  $N_{R=1}^{\text{excess}} \sim 50$  and  $N_{R=0}^{\text{excess}} \sim 30$ . From these results it is clear that active objects are not typically located in moderately rich galaxy enhancements such as Abell  $R = 0$  clusters, as suggested in previous works (see for instance Smith et al. 1999, Mc. Lure & Dunlop 2000).

### 3.2 Distribution of $b_J - R$ colour indexes of neighbouring galaxies

The relative fraction of different stellar populations in galaxies are reflected in the  $b_J - R$  colour index. Elliptical galaxies, dominated by an old population of stars, have typical values  $b_J - R \sim 1.5 - 2$ , while in late types with recent episodes of star formation,  $b_J - R < 1$ . In this subsection we explore the properties of the stellar populations of galaxies in the vicinity of the different target samples using  $b_J - R$  colour indexes. We study the normalised distribution of  $b_J - R$  of APM galaxies around the targets within a projected distance  $r_p < 0.5h^{-1}\text{Mpc}$ . We adopt the same limiting apparent magnitude  $b_J^{\text{lim}} = 20.5$  for all tracer samples and we compute:

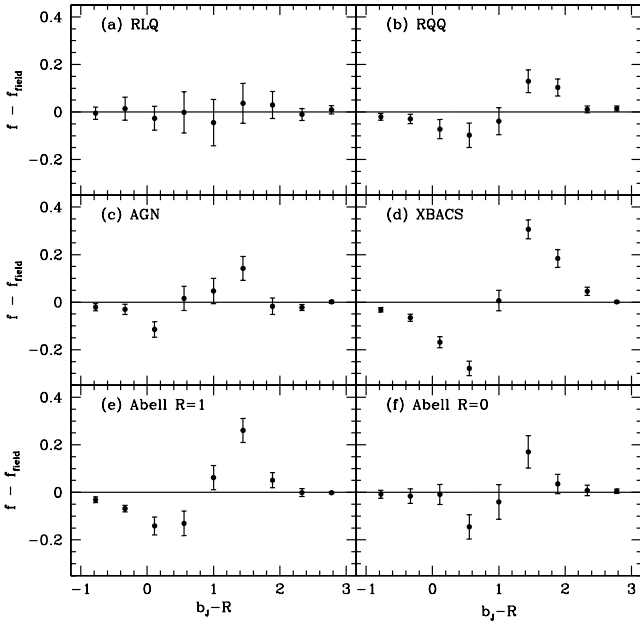
$$f(b_J - R) = \frac{N(b_J - R)}{N^{TOT} \Delta(b_J - R)}, \quad (6)$$

where  $N(b_J - R)$  is the number of APM galaxies with colour indexes in the interval defined by  $[(b_J - R) - \Delta(b_J - R)/2, (b_J - R) + \Delta(b_J - R)/2]$ , and  $N^{TOT}$  is the total number of APM galaxies within  $r_p \leq 0.5h^{-1}\text{Mpc}$ . Error bars in these distributions were computed using the bootstrap resampling technique. We subtract from these distributions the colour distribution of tracer galaxies in the randomly selected fields. The results are displayed in Figure 3. As it is expected from the well known morphology-density relation (Dressler 1980), there is a marked relative excess of early ( $1 \leq b_J - R \leq 2$ ) to late type galaxies ( $0 \leq b_J - R \leq 1$ ) within  $r_p \leq 0.5h^{-1}\text{Mpc}$  for the three samples of clusters, an effect that is stronger for the richer cluster samples. Active objects show a weaker tendency, although, the distribution of colours of RQQs shows a similar excess of red galaxies than in  $R = 0$  clusters. For RLQs, the signal for the presence of a red galaxy population is almost negligible, while AGNs show an intermediate behavior between RQQs and RLQs.

To quantify the previous results, we have computed a parameter  $\mathcal{P}$  that characterizes the relative fraction of red to blue galaxies in a given range of projected separations

**Table 2.**  $\mathcal{P}$  parameter for the different target samples within three projected distances.

Sample	$\mathcal{P}$	$\mathcal{P}$	$\mathcal{P}$
	$r_p \leq 0.3h^{-1}\text{Mpc}$	$r_p \leq 0.5h^{-1}\text{Mpc}$	$r_p \leq 1h^{-1}\text{Mpc}$
RQQs	$0.10 \pm 0.06$	$0.09 \pm 0.04$	$0.07 \pm 0.02$
RLQs	$-0.22 \pm 0.08$	$-0.05 \pm 0.07$	$-0.05 \pm 0.04$
AGNs	$0.08 \pm 0.05$	$0.03 \pm 0.04$	$-0.01 \pm 0.02$
XBACS	$0.49 \pm 0.03$	$0.38 \pm 0.02$	$0.30 \pm 0.02$
Abell $R = 1$	$0.17 \pm 0.05$	$0.20 \pm 0.04$	$0.16 \pm 0.02$
Abell $R = 0$	$0.18 \pm 0.07$	$0.09 \pm 0.04$	$0.06 \pm 0.02$
Field	$-0.11 \pm 0.01$		

**Figure 3.** Colour index  $b_J - R$  distributions normalised to randomly selected fields corresponding to galaxies within  $r_p \leq 0.5h^{-1}\text{Mpc}$  from the targets.

$$\mathcal{P} = \frac{N_R - N_{b_J}}{N_R + N_{b_J}}, \quad (7)$$

where  $N_R$  is the number of neighbour tracer galaxies in the range  $1 \leq b_J - R \leq 2$  and  $N_{b_J}$  is the number in the range  $0 \leq b_J - R \leq 1$ . In Table 2 we list this parameter for three projected distance ranges ( $r_p \leq 0.3h^{-1}\text{Mpc}$ ,  $r_p \leq 0.5h^{-1}\text{Mpc}$  and  $r_p \leq 1h^{-1}\text{Mpc}$ ) and their corresponding bootstrap resampling uncertainties estimates.

The values of  $\mathcal{P}$  in Table 2 allow us to quantify and extend the previous results of this subsection. By inspection to this table it can be seen that galaxies in clusters show the tendency of systematically larger colour indexes near the center. The population of galaxies in the neighbourhood of RQQs have  $\mathcal{P}$  comparable to that of galaxies in  $R = 1$  and  $R = 0$  Abell clusters. It is worth to notice the negative values of  $\mathcal{P}$  for galaxies in the vicinity of RLQs which indicate the lack of a red galaxy population, characteristic of high density regions, around these objects. In order test the stability of these results we have changed the boundaries adopted to

calculate the values of  $\mathcal{P}$ . The analysis shows that the above conclusions are robust and do not depend on the particular choice of colour boundaries in the calculations, provided the parameter  $\mathcal{P}$  reflects the relative fraction of early-type to late-type galaxies.

## 4 DISCUSSION

The results discussed previously lead us to conclude that quasars and AGNs are not placed in galaxy density enhancements corresponding to rich and moderately rich clusters of galaxies. As it can be clearly appreciated by inspection to Figure 2, the galaxy overdensity around these center targets is significantly lower than that corresponding to Abell  $R = 1$  or  $R = 0$  clusters of galaxies. Thus, active objects are more likely to reside in groups (typically 10 neighbours with  $M_{b_J} \leq M_{b_J}^* + 2$  within  $r_p \leq 1h^{-1}\text{Mpc}$ ). It has been often argued that quasar environment correspond to that of moderately rich clusters, our results indicate that active nuclei reside in regions of at most half the projected galaxy density of  $R = 0$  clusters.

The distribution of  $b_J - R$  colour indexes of galaxies within projected distances  $r_p \leq 1h^{-1}\text{Mpc}$  centered on RLQs is significantly different than that corresponding to clusters. This fact suggests that the stellar population of the neighbouring galaxies of RLQs differs significantly from that in rich and moderate galaxy density enhancements. The environments of RQQs show  $b_J - R$  colour indexes similar to galaxies in clusters while AGNs show an intermediate behavior.

We find statistical evidence that the distribution of  $b_J - R$  colours of galaxies in the vicinity of radio-quiet and radio-loud quasars are different. The latter have a population of neighbouring galaxies with lower values of colour indexes. This fact should be considered in models of the effects of nuclear activity on galaxy formation and evolution.

## 5 ACKNOWLEDGMENTS

We thank Dr. Howard Yee for useful comments. We are indebted to Dr. Carlton Baugh for reading the manuscript and providing helpful suggestions. The authors would like to thank the anonymous referee for helpful comments that improved the previous version of this paper.

This research was partially supported by grants from

CONICET, Agencia Córdoba Ciencia, Secretaría de Ciencia y Técnica de la Universidad Nacional de Córdoba and Fundación Antorchas, Argentina.

## REFERENCES

- Abell G.O., Corwin Jr. H.G. & Olowin R.P., 1989, ApJS, 70, 1A.  
Babul, A., & White, S. D. M., 1991, MNRAS, 253, 31p.  
Barrow, J. D., Bhavsar, S. P., & Sonoda, B. H., 1984, MNRAS, 210, 19p.  
Baugh, C. M. & Efstathiou, G., 1993, MNRAS, 265, 145.  
Best, P. N., 2000, MNRAS, 317, 720.  
Dressler, A., 1980, ApJ, 236, 351.  
Ebeling, H., Voges, W., Böhringer, H., Edge, A. C., Huchra, J. P. & Briel, U. G., 1996, MNRAS, 281, 799.  
Fischer, K. B., Bahcall, J. N. Kirhakos, S. & Schneider, D. P., 1996, ApJ, 468, 469.  
Lilje, P. B. & Efstathiou, G., 1988, MNRAS, 231, 635.  
Martínez, H. J., Merchán, M. E., Valotto, C. A. & Lambas, D. G., 1999, ApJ, 514, 548.  
Mc. Lure, R. J. & Dunlop, J. S., 2000, astro-ph/0007219.  
Rees, M. J., 1988. In: *Large Scale structure in the Universe, IAU Symp. No. 130*, p. 437, eds Audouze, J., Pelletan, M. C. & Szalay, A. S., Kluwer, Dordrecht.  
Schechter, P. L., 1976, ApJ 203, 297.  
Silk, J. & Rees, M. 1998, A&A, 311, 1.  
Smith, R. J., Boyle, B. J., & Maddox, S. J., 1995, MNRAS, 277, 270.  
Smith, R. J., Boyle, B. J., & Maddox, S. J., 1999, astro-ph/9911400.  
Toomre, A. & Toomre, J. 1972, ApJ, 178, 623.  
Véron-Cetty M. P. & Véron, P., 2000, Quasars and Active Galactic Nuclei (9th Ed.), ESO Scientific Report 19.  
Voit, M. 1996, ApJ, 465, 568.  
Wold, M., Lacy, M., Lilje, P. and Serjeant, S., 2000, MNRAS, 316, 267.  
Wold, M., Lacy, M., Lilje, P. and Serjeant, S., 2001, MNRAS, 323, 231.  
Yee, H. K. C., & Green, R. F. 1987, ApJ, 319, 28.  
Yee, H. K. C. 1990 Evolution of the Universe of Galaxies, ASP Conference Series, Vol. 10, p. 322 (San Francisco: BookCrafters, Inc.).